# RSC Advances

## RSC Advances

www.rsc.org/advances

ROYAL SOCIETY
OF CHEMISTRY

www.rsc.org/advances
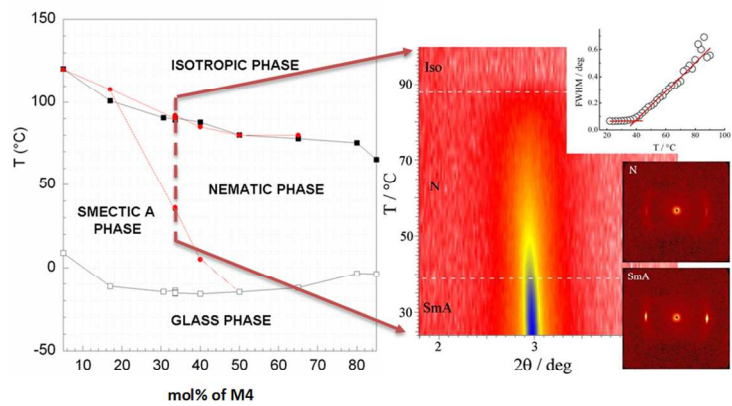
338x190mm (96 x 96 DPI)

# Effect of co-monomers' relative concentration on self-assembling behaviour of side-chain liquid crystalline elastomers

*Valentina Domenici[1*], Jerneja Milavec[2], Alexej Bubnov[3], Damian Pociecha[4],*

*Blaž Zupančič[2], Andraž Rešetič[2], Věra Hamplová[3], Ewa Gorecka[4], Boštjan Zalar[2]*

[1] Dipartimento di Chimica e Chimica Industriale, Università degli studi di Pisa, via Risorgimento 35, 56126 Pisa, Italy

[2] Department of Solid State Physics, Jožef Stefan Institute, Jamova 39, SI-1000 Ljubljana, Slovenia

[3] Institute of Physics, Academy of Sciences of the Czech Republic, Na Slovance 2, 182 21 Prague 8, Czech Republic

[4] University of Warsaw, Department of Chemistry, Żwirki i Wigury 101, 02-089 Warszawa, Poland

**\* Corresponding author:** Valentina Domenici, Dipartimento di Chimica e Chimica Industriale, Università di Pisa, via Risorgimento 35, 56126 Pisa (Italy). Tel: 0039-050-2219215; Fax: 0039-050-2219260; E-mail: valentina.domenici@unipi.it

1

**Abstract**

This work deals with design and characterization of a new series of liquid crystalline elastomers in the form of monodomain films, showing the self-assembling behaviour, namely the nematic and the orthogonal smectic A phases. The procedure for design and preparation of monodomain and polydomain polysiloxane-based side-chain liquid crystalline elastomers containing different concentrations of two mesogenic monomers and a constant density (about 15 mol%) of the crosslinker is reported. The phase diagram and mesomorphic behaviour of new resulting liquid crystalline elastomers were determined by differential scanning calorimetry (DSC), polarizing optical microscopy (POM) and especially X-ray diffraction studies, which helped to clearly identify the smectic A phase. Among new liquid crystalline elastomer films, a specific concentration of co-mesogens gives an unconventional and fascinating system with a direct transition from the isotropic to smectic A phase. Results of the thermo-mechanic studies confirmed the shape-memory properties of these films, which have elastic properties optimal for applications as thermo-mechanic actuators.

## 1. Introduction

Liquid Crystalline Elastomers (LCEs) are soft materials having remarkable properties, such as thermo-elastic and thermo-mechanic ones, which are related to both the self-assembling properties of the mesogenic units and to the elastic response of the polymer network [1]. As a result, shape-memory behaviour of LCEs is observed when temperature crosses the transition from the isotropic to self-assembling state [2]. So far, a few technological applications based on LCEs have been proposed, from valves [3] and tweezers [4] to optical devices, such as tunable holographic gratings [5] or Braille readers [6,7,8]. However, the interest in these partially ordered materials and their possible applications is gradually growing. For instance, in the recent years, several efforts have been spent in new synthetic procedures to produce main-chain [9] and side-chain [10] liquid crystalline elastomers, by incorporation of different mesogenic units [6,11] as well as different polymer backbones [12,13]. Among them, LCEs based on polysiloxane chains are probably the most studied and known. A particular type of polysiloxane-based LCEs is the so-called Liquid Single Crystal Elastomer (LSCE), which is a monodomain oriented LCE in the form of a thin film, first prepared by Finkelmann *et al.* [14] who mastered an original design and preparation procedure based on a two-steps crosslinking; the second step being under controlled stretching.

Although most of these LSCEs exhibits a nematic (N) phase, stable over a wide temperature range [1,15], several works have been devoted to the achiral orthogonal smectic A (SmA) [11,16,17,18,19,20] and to the tilted smectic C [21,22], but also to chiral smectic C* (SmC*) elastomers [23,24]. According to two-step crosslinking procedure [14], nematic LSCE films are characterized by a specific macroscopic alignment of the local nematic director, *n*, along the stretching direction of the film (**Scheme 1a**). As for the smectic A LSCE films, the local phase director, *n*, as well as the rod-like mesogens are usually aligned along the stretching direction, while the polymer chains are aligned on average in the orthogonal direction (**Scheme 1b**). The particular

structure and alignment of main components of smectic A LSCEs determine their strong anisotropic

properties, such as elasticity [25,26] and rheology [27,28].

***Scheme 1.*** *Sketch of the structure and alignment of the basic constituents (rod-like mesogens, polymer*

*chains and crosslinkers) in a nematic LSCE (a) and a typical smectic A LSCE (b). Black arrow*

*indicates the stretching direction.*



(a)          (b)
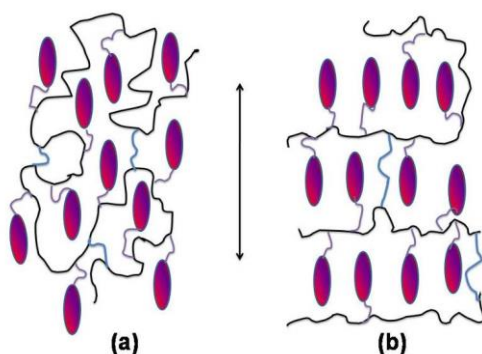
Several fascinating effects were observed on smectic A LCEs, much more pronounced than in low-

molecular-weight smectic liquid crystals, such as the electroclinic effect [29,30,31], i.e. tilting of

mesogens with respect to the smectic layer normal induced by an applied electric field. In the case of

achiral smectic A LCEs, a similar effect to the electroclinic one can be obtained without the

application of external electric field, but, instead, by applying an external shear in the orthogonal

direction with respect to the phase director. The applied shear produces a macroscopic deformation

of the film, which corresponds to a tilt of the mesogenic units, as demonstrated by a recent X-ray

study [32]. The complex relationship between molecular structure and stress-strain behaviour in

smectic LCEs stimulated several works, both theoretical and experimental ones [33,34,35,36,37,38].

Moreover, the mechanical and elastic properties as well as the spontaneous thermal contraction of

these systems can, in principle, be tuned as a function of the chemical constituents and their relative

concentrations [35].

Another peculiar phenomenon was observed at the nematic − smectic phase transition of several

LCEs, the transition from an ordered to a disordered state of the system, can be associated to the

sensitive changes in the elastic modulus and maximum elongation [36]. On contrary, very few

researches are known about LSCE systems having a direct isotropic-smectic phase transition [16,39].

In this work, we are reporting the design and detailed characterization of two rod-like monomers,

namely a nematogen, 4-methoxyphenyl 4-(but-3-en-1-yloxy) benzoate (**M4**) and a smectogen, 4-

methoxyphenyl 4-(undec-10-en-1-yloxy) benzoate (**M11**), which were used to prepare several

monodomain and polydomain polysiloxane-based side-chain LCE films (see **Fig. 1**). The

mesomorphic behaviour and self-assembling properties of monomers themselves and of the prepared

LCE system were studied by differential scanning calorimetry (DSC), polarized optical microscopy

(POM), small angle and wide angle X-ray diffraction. Moreover, the thermo-mechanic behaviour and

elastic modulus of the LCEs were also studied in view of new applications in actuator micro-systems.

**Fig. 1.** *Chemical constituents of the LCE films: (a) polymer chain; (b) nematogen **M4**; (c) smectogen **M11** and
(d) crosslinker **V1**.* X *stands for* $^1H$, *i.e. for non-labelled compounds.*



5
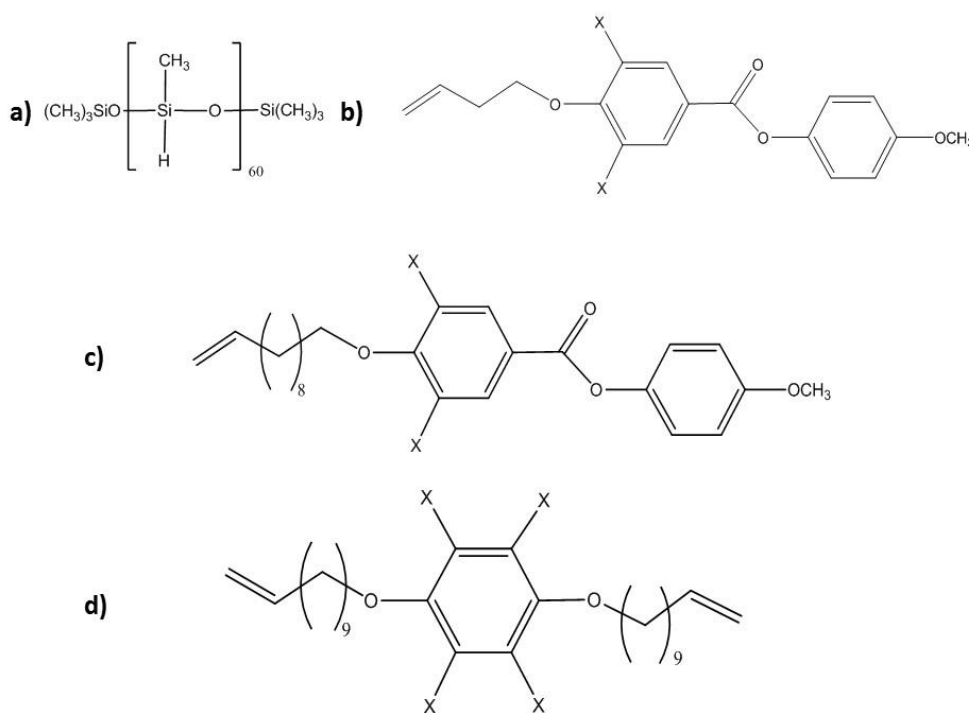
## 2. Experimental section

### *2.1 Synthesis of the mesogenic monomers*

Synthesis of mesogens 4-methoxyphenyl 4-(but-3-en-1-yloxy) benzoate (**M4**) and 4-methoxyphenyl 4-(undec-10-en-1-yloxy) benzoate (**M11**) (see **Fig. 1**), have been carried out according to the synthetic route presented in Ref. [40,41]. Purification of the compounds was done by column chromatography on silica using 99.9 % of $CH_2Cl_2$ and 0.1% acetone as a mobile phase followed by recrystalization from ethanol. The yield was 85% and 80% for the **M4** and **M11** compounds, respectively. After that the compounds with purity of 99.9 % was obtained (checked by HPLC, which was carried out using a silica gel column Bioshere Si 100-5$\mu$m, 4x250, Watrex with a mixture of 99.9 % of toluene and 0.1 % of methanol as an eluent, and detection of the eluting products by a UV-VIS detector $\lambda$ = 290 nm).

The structures of all final compounds were confirmed by ^{1}H-NMR (300 MHz, Varian):

^{1}H-NMR of **M4** (CDCl$_3$): 8.12 (d, 2H, ortho to –COO); 7.10 (d, 2H, ortho to -OCO); 6.90 (dd, 4H, ortho to -OR); 5.90 (m, 1H, =CH-); 5.20 (m, 2H, CH$_2$=); 4.10 (t, 2H, CH$_2$OAr); 3.81 (s, 3H, OCH$_3$); 2.59 (q, 2H, =CH-$\underline{CH_2}$).

^{1}H-NMR of **M11** (CDCl$_3$): 8.14 (d, 2H, ortho to –COO); 7.10 (d, 2H, ortho to -OCO); 6.90 (dd, 4H, ortho to -OR); 5.81 (m, 1H, =CH-); 4.98 (m, 2H, CH$_2$=); 4.00 (t, 2H, CH$_2$OAr); 3.81 (s, 3H, OCH$_3$); 2.05 (q, 2H, =CH-$\underline{CH_2}$); 1.80 and 1.20 (m+m, 14H, CH$_2$).

The mesomorphic behaviour of **M4** and **M11** monomers was investigated by POM and DSC, and the summary of phase transitions and calorimetric data are reported in **Table 1**. On cooling from the isotropic phase, **M4** monomer possesses the nematic phase only. However, **M11** monomer possesses the orthogonal smectic A phase below the nematic phase.

*Table 1. Sequence of phases, phase transition temperatures ($^{o}C$) measured on cooling (5K min$^{-1}$), melting points, m.p. ($^{o}C$), clearing points, c.p. ($^{o}C$) measured on heating (5K min$^{-1}$), and related phase transition enthalpies [ΔH] (Jg$^{-1}$) determined by DSC for the mesogenic monomers.*

| | m.p. | c.p. | phase | | phase | | phase | | phase |
|-----|--------|--------|-------|--------|------|--------|---|--------|-----|
| M4 | 77.6 [+102.9] | 77.6 [+102.9] | Cr | 15.5 [-70.5] | – | | N | 51.7 [-1.6] | Iso |
| M11 | 69.7 [+103.5] | 73.4 [+2.0] | Cr | 29.8 [-74.7] | SmA | 44.4 [-2.3] | N | 72.4 [-2.6] | Iso |

## 2.2 Preparation of the liquid crystalline elastomers

The two-step crosslinking ''Finkelmann procedure'' [14] has been followed in order to produce several monodomain side-chain LSCE films with various concentrations of **M4** and **M11**, and by using a crosslinking density of about 15 mol%, which was found to be optimal based on previous studies [42,43,44]. The main components of these films are reported in **Fig. 1** and the relative composition of the LSCE samples investigated in this paper is shown in **Table 2**.

The synthesis of the flexible crosslinker, **V1**, is reported elsewhere [45].

The LSCE films were prepared as follows. A pre-polymerization mixture was prepared by adding to 2.5 ml of anhydrous toluene: the poly(methylhydrosilane) (2 mmol), the crosslinker **V1** (c % mmol), the mesogen **M4** (m4 % mmol) and the mesogen **M11** (m11 % mmol), with 2c + m4 + m11 = 100 % mmol. A solution of Pt-catalyst (COD from Wacker Chemie) in $CH_2Cl_2$ is added and the pre-polymerization mixture is finally filtered.

The mesomorphic behaviour of the LCE samples was explored by combining different experimental techniques, such as DSC, POM and X-ray scattering. The results of the study are summarized in **Table 2** and discussed in **Section 3**.

7

*Table 2. List of the LSCE samples with the relative percentage concentrations (mol%) of co-monomers (**M4**, **M11**) and crosslinker **V1** together with the results on sequence of phases, phase transition temperatures T ($^o$C) measured on cooling (10K min$^{-1}$), $T_g$ ($^o$C), and related phase transition enthalpies [ΔH] (Jg$^{-1}$) as determined by DSC for all studied LCEs.*

| LCE name | Co-monomer M4 [mol%] | Co-monomer M11 [mol%] | Crosslinker V1 [mol%] | T$g$ | phase | T | phase |
|---|---|---|---|---|---|---|---|
| **LCE 80/05** | 80.0 | 5.0 | 15.0 | -3.5 [0.33] | **N** | 75.4 [-1.5] | **Iso** |
| **LCE 65/20** | 66.3 | 19.3 | 14.5 | -12.3 [0.42] | **N** | 78.0 [-2.0] | **Iso** |
| **LCE 50/35** | 50.0 | 35.0 | 15.0 | -14.8 [0.43] | **N** | 80.2 [-2.0] | **Iso** |
| **LCE 40/45** | 38.2 | 47.6 | 14.9 | -15.9 [0.59] | **N** | 87.9 [-4.6] | **Iso** |
| **LCE 34/52** | 33.6 | 51.4 | 15.0 | -15.4 [0.41] | **N** | 90.5 [-2.2] | **Iso** |
| **LCE 17/68** | 17.0 | 68.0 | 15.0 | -11.5 [0.56] | **SmA** | 100.9 [-1.9] | **Iso** |
| **LCE 05/80** | 4.7 | 81.1 | 14.2 | 9.0 [0.46] | **SmA** | 120.4 [-6.6] | **Iso** |

The first step of the reaction is carried out in a special form under centrifugation (with a spinning rate from 4500 to 6000 rpm) at T=333 K. After a period of centrifugation (typically 1–1.5 h), a partially crosslinked, gel-like film network of dimensions about 2*20 cm$^2$ and thickness of about 150 mm was obtained. The second step of reaction is performed by mechanically loading portions of the gel-like film with increasing weights (up to 2.5 g) at room temperature and then completing the crosslinking reaction in the oven at 338 K. During this second step, uniform uniaxial alignment of the films is reached with the local director oriented along the direction of the weight-controlled external stress. Monodomain stripes as well as polydomain samples were made for all LCE films and are indicated in **Table 2**. Polydomain samples were prepared without mechanically loading the gel films during the second crosslinking step.

### 2.3 Experimental techniques

8

Sequence of phases and phase transition temperatures of mesogens were determined on heating/cooling to/from the isotropic phase by identification of characteristic textures and their changes observed in the polarizing optical microscope (POM) NICON ECLIPSE E600POL. The LINKAM LTS E350 heating stage with TMS 93 temperature programmer was used for the temperature control, which enabled temperature stabilization within 0.1 K.

Phase transition temperatures and transition enthalpies of both mesogens and LCEs were evaluated from differential scanning calorimetry (DSC), Pyris Diamond, PerkineElmer 7, on cooling and heating the sample at a rate of 10 K min$^{-1}$. The sample (10 mg) hermetically sealed in aluminium pan was placed in a nitrogen atmosphere. The temperature was calibrated on extrapolated onsets of melting points of water, indium and zinc. The enthalpy change was calibrated on enthalpies of melting of water, indium and zinc. Several heating/cooling runs were performed showing a perfect reproducibility of the DSC curves.

Small-angle X-ray diffraction studies were conducted using Bruker NanoStar system (CuK$\alpha$ radiation, cross-coupled Goebel mirrors, three pinhole collimation system, MRI heating stage and Vantec-2000 area detector). XRD patterns in wide angle range were collected with Bruker GADDS system (CuK$\alpha$ radiation, Goebel mirror, point beam collimator system, modified Linkam heating stage, Vantec-2000 area detector). Samples of LCE were measured in transmission mode.

Thermo-mechanic measurements of the monodomain LCEs have been performed on a home-built computer-controlled setup comprising a temperature-controlled cell, a strain gauge, and a linear actuator for stretching the samples, which allowed for simultaneous measurement of temperature, force and sample length. The variations of the film length were recorded as a function of temperature at different heating/cooling rates by using a constant-force feedback loop with a minimal force of about 1 mN. The same apparatus has been used to measure the elastic modulus by stretching the LSCE films and simultaneously recording the applied stress.

## 3. Results and Discussions

### 3.1 Mesomorphic behaviour of monomers

The mesomorphic behaviour of the samples **M4** and **M11** was investigated by means of DSC and POM techniques and the results are summarized in **Table 1**. Microphotographs of the characteristic textures obtained at different temperatures using POM for two monomers are shown in **Fig. 2**.

**Fig. 2.** *Optical microphotographs of co-monomers: (a) nematic droplets at the Iso-N phase transition (51ºC) for **M4**; (b) nematic marbled texture (45ºC) for **M4**; (c) Phase transition from the nematic phase (on left) to the crystal phase with typical lancets (25ºC) for **M4**; (d) nematic texture with $\pi$ disclination lines (70ºC) for **M11**; (e) fan shaped texture of the smectic A phase (40ºC) for **M11**; (f) texture after crystallization (25ºC) for **M11**. Width of the microphotographs is about 300 μm.*
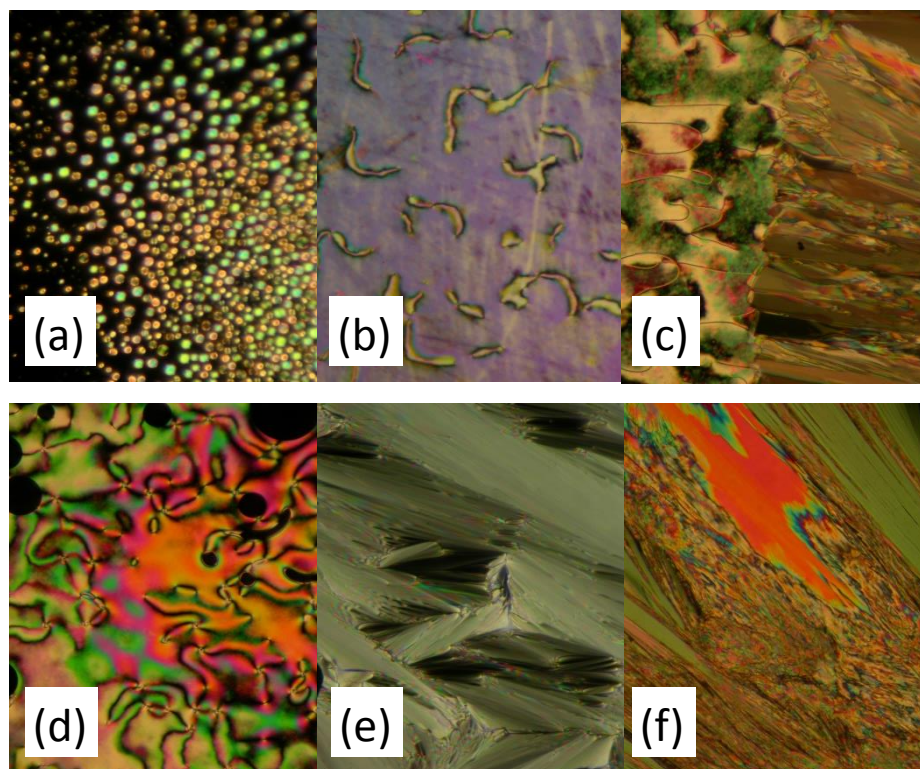


Compound **M4** has a nematic phase stable over about 30° degrees and typical textures are reported in **Fig. 2a** and **Fig. 2b**, while the monomer **M11** possesses the nematic phase (**Fig. 2d**) and a smectic

A (**Fig. 2e**) phase at lower temperature. The transition to the crystal phase occurs at about 15ºC and 30ºC for monomers **M4** and **M11**, respectively.

### *3.2 Mesomorphic behaviour of LCEs*

The LCE samples prepared with different relative concentration of mesogens **M4** and **M11** are listed in **Table 2**. As previously mentioned, the samples were in the form of film, transparent in the case of monodomain samples, and opaque in the case of polydomain ones. The mesomorphic properties of all samples were first explored by DSC and the results are summarized in **Table 2**. For **M4** and **M11** monomers the reproducibility of the repeated heating/cooling cycles was very good indicating no the absence of polymerization. Excellent reproducibility of the DSC curves (**Fig. 3**) in consecutive heating–cooling cycles was obtained for all samples, evidencing high thermal stability of the prepared LCEs. Moreover, no difference between the monodomain and polydomain samples has been detected by DSC in the values of the phase transition temperatures, as expected [1].

Typical shape of DSC curves for LCE samples is shown on **Fig. 3b** and **3c**. A peak corresponding to the isotropic - nematic phase transition and a step corresponding to the glass transition can be easily observed (**Fig. 3b** and **3c**). For comparison, the DSC of one of the monomer, namely **M11**, is also reported (**Fig. 4a**). A first identification of the mesophases formed by LCEs was done by optical texture observations using POM which was not enough to determine the mesophase. As an example, typical textures obtained in POM on **LCE 34/52** thin sample are shown in **Fig. 4**. The absence of homogeneous pattern in the isotropic phase (**Fig. 4a**) is due to the polydomain sample structure used for the purpose. Final determination of the mesophase nature came from X-Ray Diffraction (XRD) measurements performed for several samples.

11

*Fig. 3. Examples of the DSC plots on heating/cooling runs (indicated by horizontal arrows) for monomer **M11** (a) and LCE samples: **LCE 40/45** (b) and **LCE 05/35** (c). Phase transitions are indicated by vertical arrows.*
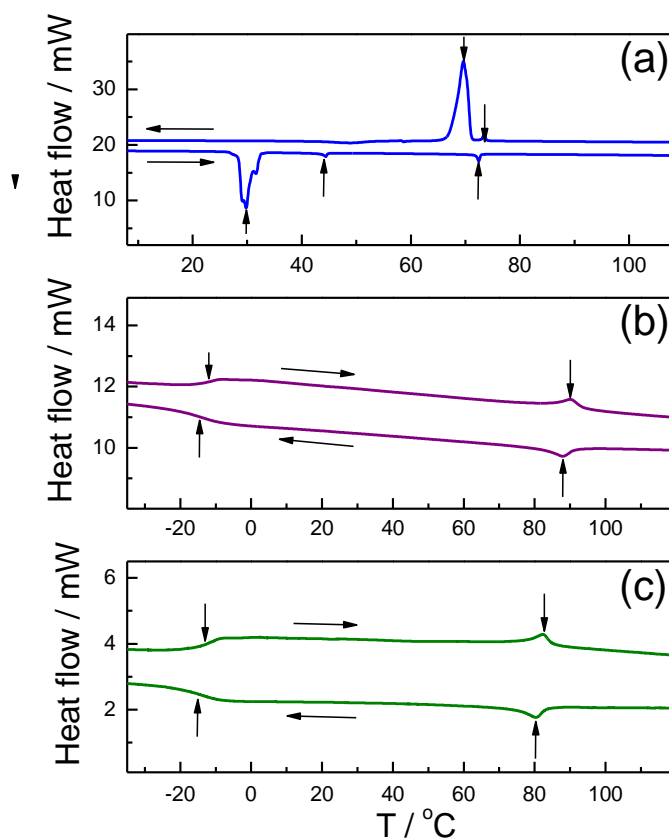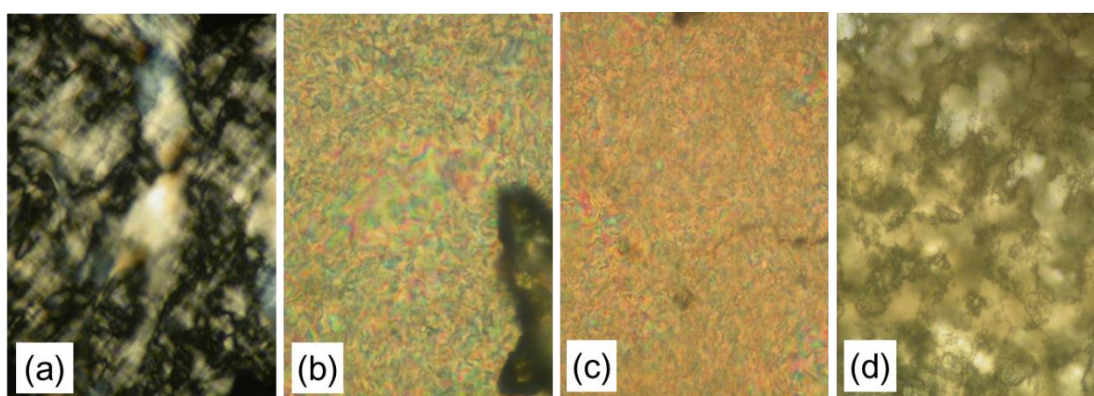


*Fig. 4. Microphotographs of textures obtained on **LCE 34/52** film: (a) at 95$^o$C; (b) at 87$^o$C; (c) at 60$^o$C; (d) about 0$^o$C. Width of the microphotographs is about 250 μm.*



For liquid crystal elastomers with low concentration of **M11** (below 50 mol%) exclusively a nematic phase was observed (see, for instance, in **Fig. 5a** and **5c**), while those with high concentration of **M11** (above 80 mol%) exhibited only the SmA phase (**Fig. 5b** and **5d**). Here, both 2D XRD patterns (**Fig.**

12

**5a** and **5b**) and the diffracted intensity *vs.* scattering angle (**Fig. 5c** and **5d**) obtained by integration of above patterns over azimuthal angle are presented. These patterns clearly show two different phases, namely the nematic and smectic A ones. The X-ray diffraction patterns for both the SmA and nematic phases exhibit few harmonic of the low angle signal (**Fig. 5**), pointing to strongly non-sinusoidal electron density profile along the director, that is due to the presence of the siloxane polymer main chain between layers of mesogenic units.

For LSCE samples with intermediate relative concentration of **M4** and **M11** (see, for instance, samples **LCE 34/52** and **LCE 40/45**) the XRD proved the transition from the nematic to smectic A phase (**Fig. 6**), which was not observed by DSC and POM. DSC curves (**Fig. 3b** and **3c**) clearly show the first high temperature transition (from isotropic to nematic), but no other phase transition has been observed. This is quite common especially for second order transitions [46].

**Figure 6** shows the small angle X-ray scattering 2D pattern as a function of temperature for the **LCE 34/52** monodomain sample. It can be seen that the intensity of the signal (shown by the change of colours in **Fig. 6**) increases smoothly passing from the nematic to the SmA phase. However, the 2D small angle XRD patterns, shown in **Fig. 6**, on the right bottom side, clearly indicate the typical pattern of the nematic and SmA phases, respectively. In fact, while in the nematic phase, the larger peaks are rather diffuse, in the case of the SmA phase, there are two sharp spots, orthogonal with respect to the orientation of the sample, indicating the presence of a smectic order.

The occurrence of a transition between the nematic and the SmA phases is also confirmed by the temperature dependence of the spectral line-width (FWHM) of the diffraction peak, as reported in the inset, on the top side, in **Fig. 6**. The change in the slope of the FWHM allowed us to determine the temperature transition with more precision. Moreover, the X-ray diffraction patterns for both the SmA and nematic phases showed few harmonic of the low angle signal (**Fig. 6**), pointing to strongly non-sinusoidal electron density profile along the director, that is due to the presence of the siloxane polymer main chain between layers of mesogenic units.

The XRD experiments performed allowed to determine the temperature dependence of the distance
$d(T)$, which corresponds to the layer thickness in case of the SmA phase and to a mean intermolecular
distance along director in case of the nematic phase (**Fig. 7**). It was observed that the $d$ value is linearly
dependent on **M11** monomer concentration in a polymer. For elastomers forming exclusively the
SmA phase, the layer spacing grows slightly on cooling, while for other samples it slightly decreases.
Interestingly, at the transition from nematic to SmA phase no jump in $d(T)$ curve has been found.

*Fig. 5* *2D XRD patterns recorded at room temperature for (a) nematic phase of* ***LCE 50/35*** *and (b) SmA phase
of* ***LCE 17/80*** *elastomers. In (c) and (d) the related diffracted intensity vs. scattering angle obtained by
integration of above patterns over azimuthal angle.*
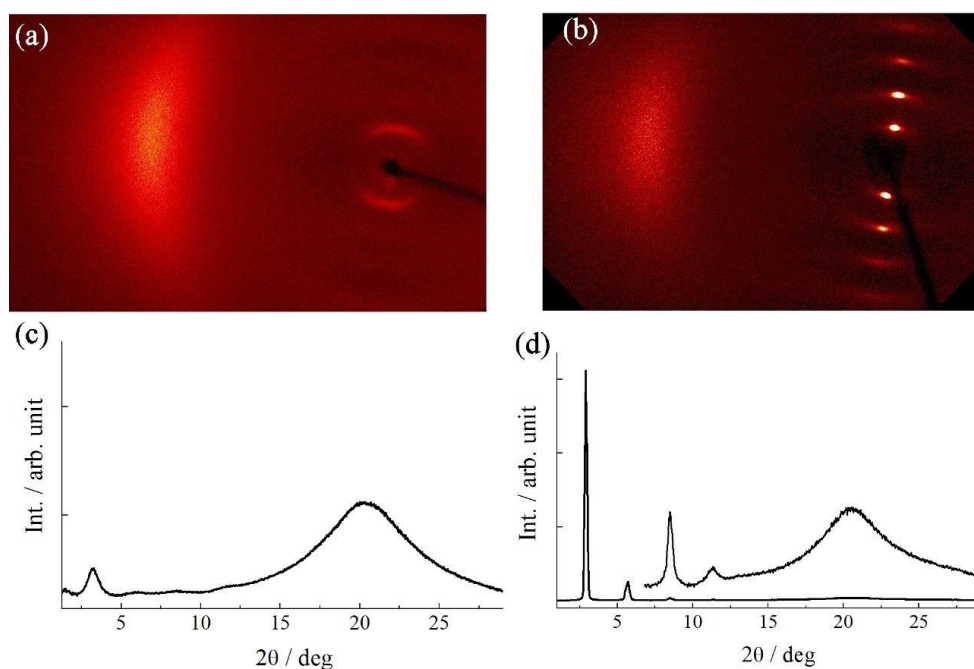


The N-SmA phase transition was accompanied by continuous narrowing of the diffraction signal at
low angles, which reflects growing correlation length for lamellar ordering at second order transition.
For monodomain elastomer samples the analysis of the azimuthal width of high angle diffraction
signal allowed for determination of orientational order parameter (S) of the mesogenic units in the
LCE [47]. For **LCE 34/52**, the obtained value S=0.71±0.05 is close to that observed for smectic the

SmA phase of **M11** monomer. Apparently, the polymerization process does not increase significantly the orientational order of mesogenic units.

*Fig. 6. Temperature evolution of SAXS pattern for **LCE 34/52** monodomain sample. Diffracted intensity is coded with colour (red to yellow to blue). In the inset, on the top side, the spectral line width (FWHM) is reported as a function of temperature. Typical small angle XRD patterns in the nematic and SmA phases are also given on right bottom side.*
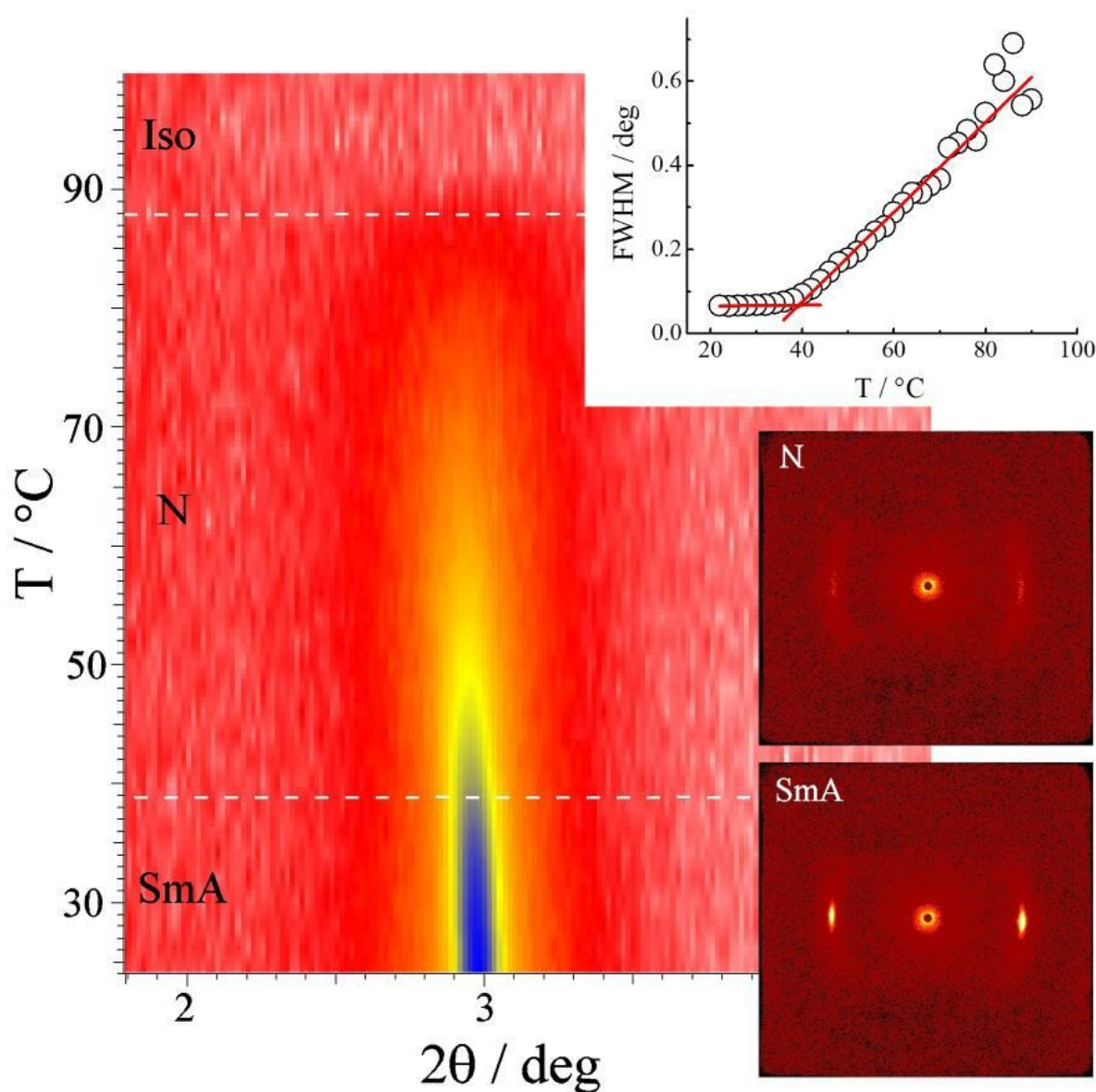
Based on experimental results shown above, a phase diagram for the studied elastomer system can be created, as reported in **Fig. 8**. The increase in **M11** co-monomer concentration, results in an increase of the clearing temperature, from ~65°C, for elastomer with only **M4** mesogen (data are from ref. [44]), to ~120°C, for elastomer with 80 mol% of **M11** co-monomer and 5 mol% of **M4** co-monomer. The glass transition temperature exhibits a minimum for samples with 40 mol% of **M4** (and 45 mol% of **M11**), and it is in almost all cases below 0°C.

*Fig. 7. Temperature dependence of the d value, which is layer spacing in smectic A phase (open symbols) and mean intermolecular distance along director in nematic phase (solid symbols) for elastomers with various concentration of mesogenic monomers: **LCE 05/80** (black circles), **LCE 17/68** (red squares), **LCE 34/52** (green triangles), **LCE 40/45** (blue circles), **LCE 50/35** (orange squares). In the inset d value at room temperature plotted versus concentration of **M11** co-monomer in LCE. Line is only a guide for eyes.*
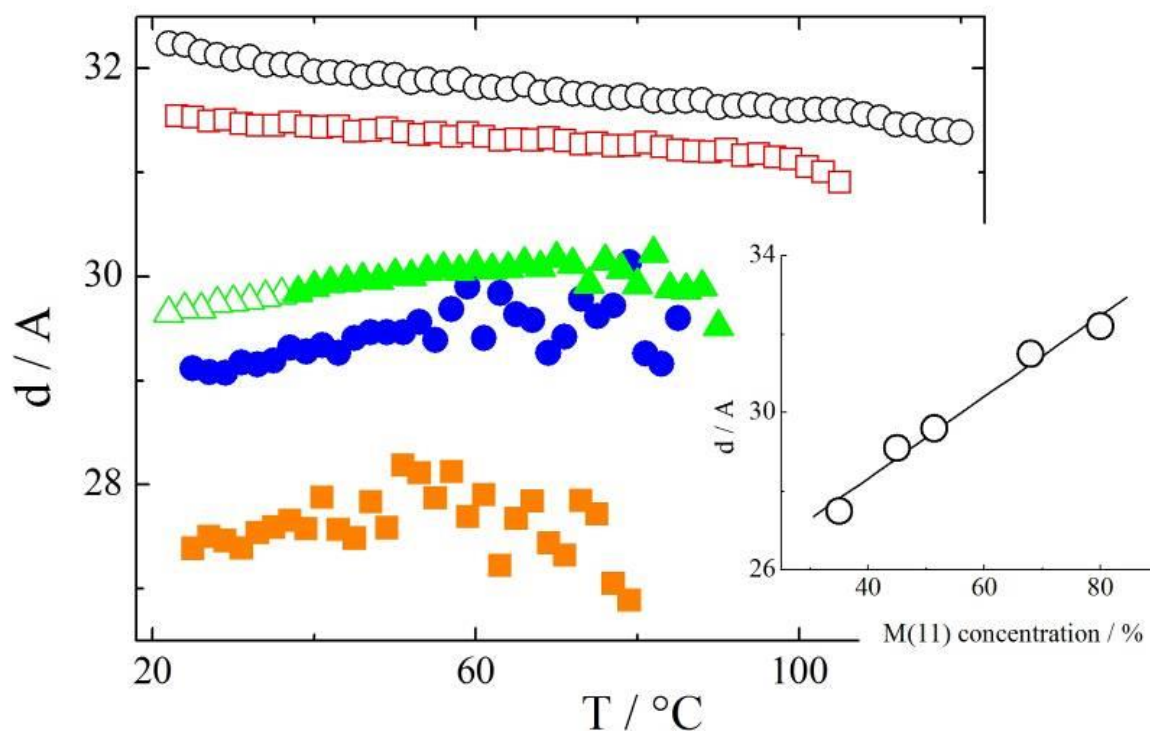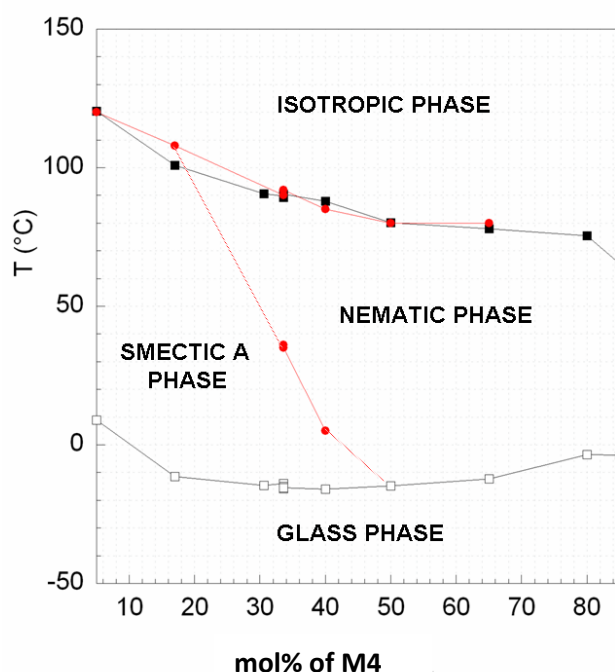
*Fig. 8. Phase diagram of the series of LCE with variable mesogenic components. Red circles refer to data obtained from X-ray and black symbols were obtained from DSC. Full and empty black squares refer to the isotropic-mesophase and mesophase-glass transitions, respectively.*

### 3.3 Thermo-mechanic and elastic properties of LCEs

For technological applications it is very essential to check the mechanical and elastic properties of the new LCE systems. Thermo-mechanical behaviour was investigated on the LCE samples in the form of thin monodomain films, as described in the Experimental Section. The elongation $\lambda = L/L_0 - 1$) of the LCE samples as a function of the temperature was greatly reproducible after several cycles and the temperature dependences of $\lambda$ $(T)$ are typical of LCE systems [1]. In LCE films possessing the nematic phase the maximum elongation was found for **LCE 80/05**, as reported in **Fig. 9(a)**, and it is about 55%.

The increase of the relative concentration of **M11** co-monomer shifts the nematic-isotropic transition to higher temperatures, as it has been already shown at the phase diagram (**Fig. 8**). However, it also results in a decreasing of the maximum elongation, which is a bit more than 30% in the **LCE 34/52** sample (**Fig. 9(a)**).

In two cases, namely the **LCE 34/52** and **LCE 40/45** (black and red curves, respectively, in **Fig. 9**), the systems present also a transition between the nematic and the smectic A phases. From the thermo-mechanical point of view, any jump is observed at the transition. However, it can be clearly seen that the elongation remains constant, or decreases, within the SmA temperature range of stability, while in the case of the nematic phase, an increase of the elongation by decreasing the temperature is always observed (see for instance, blue and green curves in **Fig. 9**).

The thermo-mechanical behaviour of LCE films exhibiting the isotropic-smectic A phase transition is reported in **Fig. 9(b)**. In that case, the trends clearly have a more pronounced jump at the Iso-SmA phase transition, reaching about the maximum elongation in few temperature degrees. In the case of **LCE 17/68** the maximum elongation is quite high for the LCE system possessing the SmA phase, and is found to be about 33%.

*Fig. 9. Thermo-mechanic measurements on the monodomain LCE samples. (a) Samples showing the isotropic-nematic phase transition: **LCE 34/52** (black), **LCE 40/45** (red), **LCE 50/35** (blue) and **LCE 80/05** (green). (b) Samples showing the isotropic-smectic A phase transition: **LCE 17/68** (black) and **LCE 05/80** (red).*
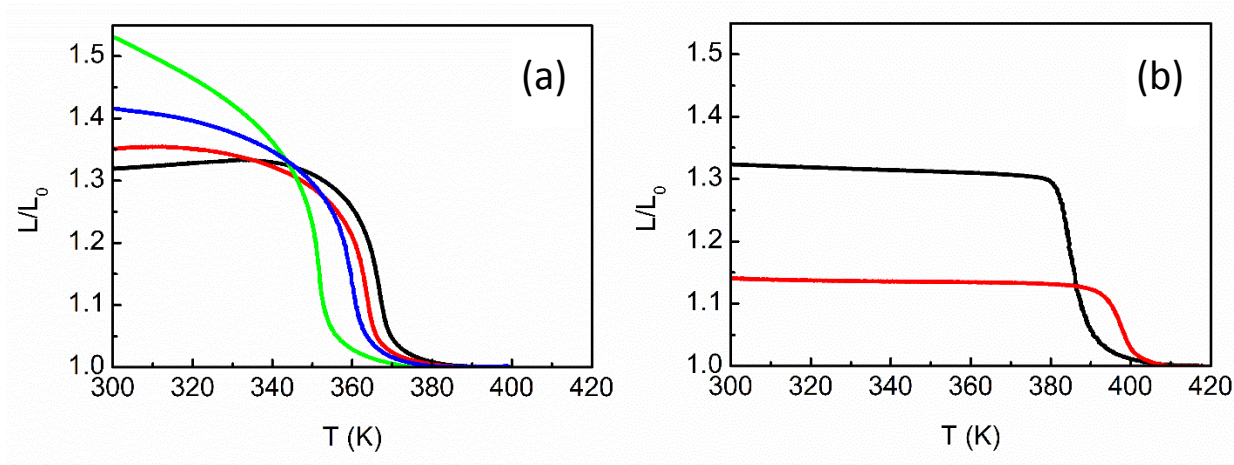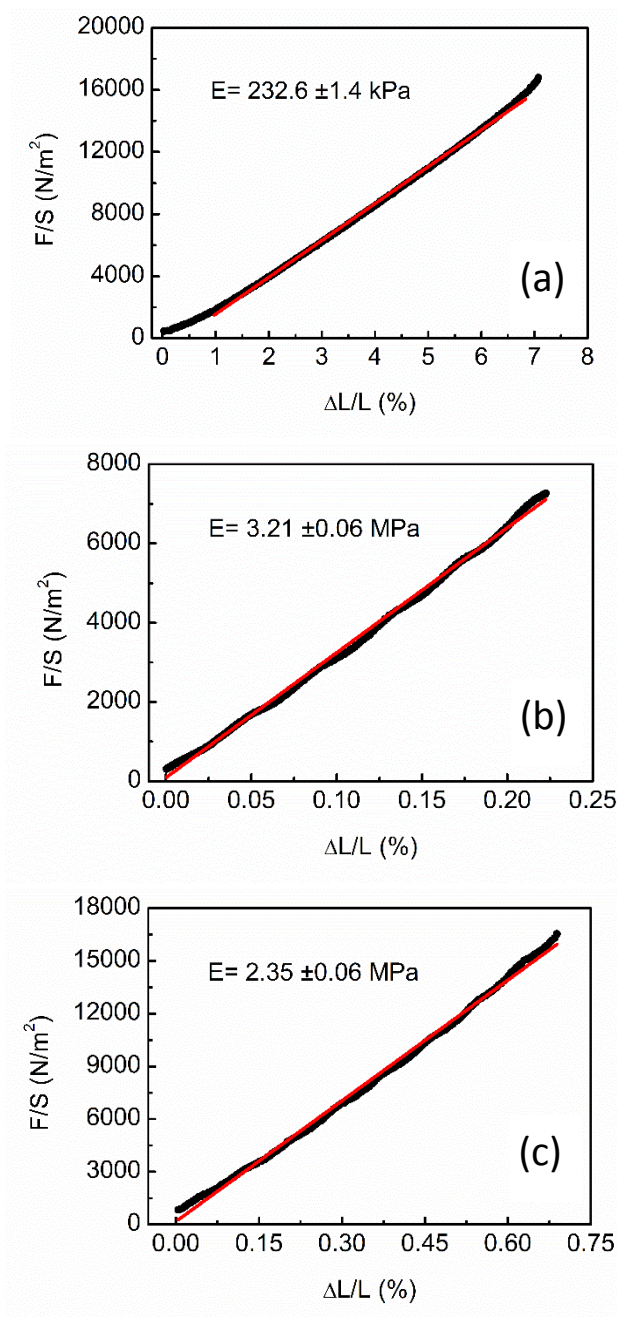
**Fig. 10.** *Elastic modulus of selected monodomain LCE samples measured at room temperature. Stretching and compression were applied at a controlled value of the force. Experimental data are in black, fitting curves are in red: (a)* **LCE 50/35**; *(b)* **LCE 17/68**; *(c)* **LCE 05/80**.



Elastic modulus of the designed LCE systems has been measured by applying uniaxial mechanical stress parallel to the director axis (**Fig. 10**). By increasing the share of **M11** co-monomer, the modulus rises from 230 kPa (a value typical for nematic LSCEs) to about 3 MPa that signifies an existence of

smectic phase. In particular, the rubber elastic response of a nematic network is replaced by the enthalpy-elastic behaviour related to the long-range one-dimensional order of smectic layers [48].

## 4. Conclusions

Series of new liquid crystalline elastomers (both the monodomain and polydomain) with siloxane backbone and two types of mesogens (co-monomers), differing in the length of terminal chains, attached to the main siloxane chain have been designed in order to investigate the effect of the chemical structure and relative concentrations of the two co-monomers on self-assembling behaviour. The systematic variation of relative concentration of shorter and longer co-monomers allows to find the specific concentration range for which the temperature induced nematic-smectic A phase transition has been detected. For all studied system it was possible to obtain macroscopic (few centimetres) monodomain samples in both nematic and SmA phases. In particular, we obtain that if the longer **M11**co-monomer is present at higher concentration than 68 mol% (with respect to the **M4** co-monomer) the new LCEs possess a direct isotropic to smectic A phase transition, while at lower concentration than 45 mol% only a nematic phase has been observed. In between, two mesophases exist and the N-SmA phase transition is of the second order, with a continuous increase of positional order of mesogens, as clearly seen by X-ray scattering studies.

The self-assembling behaviour of both co-monomers by themselves and the resulting elastomers were investigated by combining different experimental techniques, namely POM, DSC, SAXS and WAXS methods. Moreover, the thermo-mechanic and elastic properties of liquid crystalline elastomers in the form of monodomain films, both nematic and smectic ones, have been established in order to check the appropriateness of the preparation method and to explore the potential to use these new LCE materials for actuation devices.

**Acknowledgments**

## Table of Entry:
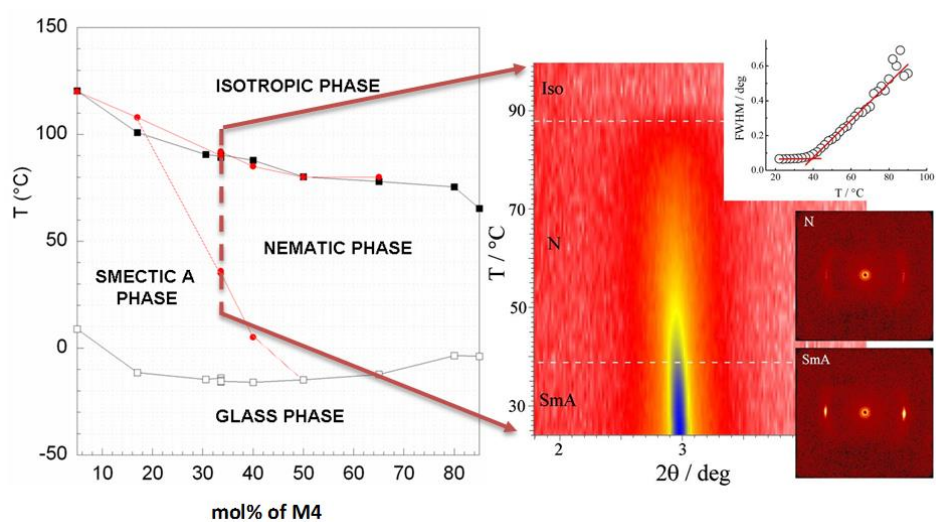


A new series of liquid single crystal elastomers having a Nematic-SmA and a direct Isotropic-SmA phase transition.

**References**

[1] Warner M, Terentjev EM. Liquid Crystal Elastomers. Oxford: Oxford University Press; 2003, 1-424.

[2] de Gennes PG. C R Acad Sci 1975; 281: 101-3.

[3] Sanchez-Ferrer A, Fischl T, Stubenrauch M, Albrecht A, Wurmus H, Hoffmann M, Finkelmann H. Adv Mater 2011; 23: 4526-4530.

[4] Sánchez-Ferrer A, Fischl T, Stubenrauch M, Wurmus H, Hoffmann M, Finkelmann H. Macromol. Chem. Phys. 2009; 210; 1671-1677.

[5] Tašič B, Li W, Sánchez-Ferrer A, Čopič M, Drevenšek-Olenik I. Macromol. Chem. Phys. 2013; 214; 2744-2751.

[6] Devetak M, Zupancic B, Lebar A, Umek P, Zalar B, Domenici V, Ambrozic G, Zigon M, Copic M, Drevensek-Olenik I. Phys Rev E 2009; 80: 050701.

[7] Camargo C, Campanella H, Marshall J, Torras N, Zinoviev H, Terentjev E, Esteve J. J Micromech Microeng 2012; 22: 075009.

[8] Torras N, Zinoviev KE, Esteve J, Sánchez-Ferrer A. Mater. Chem. C. 2013; 1; 5183-5190.

[9] Burke KA, Mather PT. Polymer 2013; 54: 2808-2820.

[10] Meng FB, Zhang XD, He XZ, Lu H, Ma Y, Han HL, Zhang BY. Polymer 2011; 52: 5075-5084.

[11] Bubnov A, Domenici V, Hamplová V, Kašpar M, Zalar B. Polymer 2011; 52: 4490-4497.

[12] Liu JH, Wang YK, Chen CC, Yang PC, Hsieh FM, Chiu YH. Polymer 2008; 49: 3938-3949.

[13] Ambrogi V, Giamberini M, Cerruti P, Pucci P, Menna N, Mascolo R, Carfagna C, Polymer 2005; 46: 2105-2121.

[14] Kupfer J, Finkelmann H. Makromol Chem Rapid Commun 1991; 12: 717-26.

[15] Toth-Katona T., Cigl M., Fodor-Csorba K., Hamplová V., Jánossy I., Kašpar M., Vojtylová T., Bubnov A., Macromol. Chem. Phys. 2014; 215: 742-752.

[16] Cordoyiannis G, Kramer D, Lavric M, Finkelmann H, Kutnjak Z. Mol Cryst Liq Cryst 2012; 553: 193-198.

[17] Kramer D, Finkelmann H. Macromol Rapid Comm 2011; 32: 1539-1545.

[18] Hiraoka K, Kishimoto T, Masayuki K. Tohru T. Liq Cryst 2011; 38: 489-493.

[19] Nishikawa E, Finkelmann H. Macromol. Rapid Commun. 1998; 19; 181-183.

[20] Nishikawa E, Finkelmann H. Macromol. Chem. Phys. 1999; 200; 312-322.

[21] Sánchez-Ferrer A, Finkelmann H. Macromolecules 2008; 41; 970.

[22] Sánchez-Ferrer A, Finkelmann H. Mol. Cryst. Liq. Cryst. 2009; 508; 348-356.

[23] Hiraoka K, Finkelmann H. Macromol Rapid Comm. 2001; 22: 456-460.

[24] Hiraoka K, Mochida K. Liq Cryst 2013; 40: 669-680.

[25] Stannarius R, Kohler R, Dietrich U, Losche M, Tolksdorf C, Zentel R. Phys Rev E 2002; 65: 041707.

[26] Adams JM, Warner M. Phys Rev E 2005; 71: 021708.

[27] Nishikawa E, Finkelmann H, Brand HR. Macromol Rapid Commun 1997; 18: 65-71.

[28] Weilepp J, Stein P, Assfalg N, Finkelmann H, Martinoty P, Brand HR. Europhys Lett 1999; 47: 508-14.

[29] Spillmann CM, Ratna BR, Naciri J. Appl Phys Lett 2007; 90: 021911.

[30] Hiraoka K, Cobias M, Kazama R, Finkelmann H. Macromolecules 2009; 42: 5600.

[31] Kohler R, Stannarius R, Tolksdorf C, Zentel R. Appl Phys Mater Sci Process 2005; 80: 381.

[32] Kramer D, Finkelmann H. Soft Matter 2011; 7: 1861-1867.

[33] Spillmann CM, Konnert JH, Adams JM, Deschamps JR, Naciri J, Ratna BR, Phys Rev E 2010; 82: 031705.

[34] Stannarius R, Aksenov V, Blasing J, Krost A, Rossle M, Zentel R. Phys Chem Chem Phys 2006; 8: 2293.

[35] Sanchez-Ferrer A, Finkelmann H. Solid State Sciences 2010; 12: 1849-1852.

[36] de Jeu WH, Ostrovskii BI, Kramer D, Finkelmann H. Phys. Rev. E 2011; 83: 041703.

[37] Brown AW, Adams JM. Phys. Rev. E 2013, 88: 012512.

[38] Sanchez-Ferrer A, Finkelmann H. Macromol. Rapid Comm. 2011, 32: 309-315.

[39] Mukherjee PK. J. Mol. Liq. 2013; 187: 266-271.

[40] Marini A, Domenici A, Malanga C, Menicagli R, Veracini CA, Tetrahedron 2010; 66: 3472 – 3477.

[41] Finkelmann H, Kiechle U, Rehage G. Mol. Cryst. Liq. Cryst. 1983; 94; 343-358

[42] Lebar A, Cordoyiannis G, Kutnjak Z, Zalar B. Advances in Polymer Science, pp. 1-39, Springer-Verlag, Berlin; 2012.

[43] Domenici V, Zalar B, Phase Transitions 2010; 83: 1014-1025.

[44] Domenici V. Progr. Nucl. Magn. Reson. Spectr. 2012; 63: 1-32.

[45] Sánchez-Ferrer A. Ph.D. Thesis: "Photo-active liquid crystalline elastomers", Facultat de Quimiques, Departament de Quimica Organica, Barcelona; 2006.

[46] Kumar S, "Liquid Crystals: Experimental Study of Physical Properties and Phase Transitions", Cambridge University Press, London: 2011.

[47] Davidson P, Petermann D, Levelut AM. J. Phys. II 1995; 5: 113.

[48] Kundler I, Nishikawa E, Finkelmann H. Macromolecular symposia. 1997; 117; 11-19.

**RSC Advances Accepted Manuscript**